FOREX Publication
Open Access | Rapid and quality publishing

International Journal of
Electrical and Electronics Research (IJEER)
Research Article | Volume 11, Issue 4 | Pages 1001-1012 | e-ISSN: 2347-470X

Innovative Approach of Spectral Efficiency Optimization over Various Pilot Reuse Factors

Nirav Patel[1*] and Vijay Patel[2]
[1]*Research Scholar, Ganpat University, nirav2009ec@gmail.com*
[2]*Assistant Scholar Ganpat University, vijay.patel@ganpatuniversity.ac.in*

***Correspondence:** Nirav Patel; nirav2009ec@gmail.com; +91 9904844121

ABSTRACT- The Massive MIMO with TDD is breakthrough technology for spectral efficiency gains. The CSI is essential for spectral efficiency gains and CSI can be obtained by channel estimation methods. The channel estimation methods employ known pilot s sequences to estimate the channel before actual data transmission. However, the channel coherence is time and frequency limited, which reflects the trade-off between the resources available for pilots and those available for data in coherent block for transmission. The pilot sequences reuse in other cells can reduce pilot overhead, called pilot reuse. However potential interference is introduced, by pilot reuse, in the channel estimation phase, called pilot contamination. The aim is to determine optimum pilot reuse factor for better SE using low computational complexity estimation method. The sum averaged SE has been obtained for pilot reuse factor 1, 2, 4, 8 and 16 using MMSE, EW-MMSE and LS channel estimation methods. The obtained results reveals that the difference between values of SEs for f=1 to f=2 to f=4 is very low and performance difference between estimators decreases as pilot reuse factor increases, which allows to use LS estimator to get performance almost equal to MMSE with less computational complexity. Also, the pilot reuse factor f=4 found optimum among all for given constraint.

Keywords: Massive MIMO, Spectral Efficiency, Channel Estimation, Pilot Reuse Factor, Inter-cell Interference, MMSE, EW-MMSE and LS.

ARTICLE INFORMATION
Author(s): Nirav Patel and Vijay Patel;
Received: 19/08/2023; **Accepted**: 21/10/2023; **Published**: 07/11/2023;
e-ISSN: 2347-470X;
Paper Id: IJEER 1908-10;
Citation: 10.37391/IJEER.110418
Webpage-link:
https://ijeer.forexjournal.co.in/archive/volume-11/ijeer-110418.html

Publisher's Note: FOREX Publication stays neutral with regard to Jurisdictional claims in Published maps and institutional affiliations.

1. INTRODUCTION

Any time-anywhere network service is becoming possible by wireless technology over the past decade. The need of higher data rates and all-time, everywhere connectivity has ignited the exponential growth in wireless cellular technology. Since past decade, the high data rate and spectral efficiency (SE) became reality due to multiple input, multiple-output (MIMO) technology in wireless communication systems. However, the MIMO technology demands increased complex processing and cost of hardware. The Massive MIMO technology evolved on demands of heavy complex processing at BS to achieve large SE gains [2]. This leads to array of hundreds of antennas at BS and tens of spatially multiplexed ser equipment (UE). Usually, the heavy traffic growth is served by wider frequency spectrum and more number of small cells deployment with dedicated BS in given area. As a result, traditional cellular networks are already densely deployed in urban areas of all countries and sub 6 GHz band is almost occupied [3]. However, in past decades, the SE growth (measured in bit/sec/Hz) was modest. As part of technological evaluation of network, the extensive improvement in SE gains is need of hour. The number of data bits transmission possible per channel use (per sample) is called SE. Also, the SE is an increasing function of the signal-to-interference-and noise ratios (SINRs) in the communication links. In practice, the intra & inter cell interference and signal attenuation are present during signal transmission in same time and frequency block, which results in SINR and SE decrement. The high gain antennas at BS can reduce signal attenuation using beam forming and interference can be reduced by scheduling UEs orthogonally in time and frequency domain. These technologies served well, but it has been changed in futuristic 5G approach for higher SE [3]. The Massive MIMO is physical layer technology used for extensive SE improvement [2]. Also, it equips each BS with an array of many active antennas to spatially multiplex many UEs on the same time-frequency resource. The advanced precoding and combining methods, called signal processing techniques, can improve SE extensively compared to traditional cellular networks. The Massive MIMO is basically a enlarged form of the space-division multiple access (SDMA) concept from the 1990s [3], with extensive spatial multiplexing and antenna array which is not before seminal paper of T. Marzetta in 2010 [4]. After that the Massive MIMO has evolved as mainstream technology into 5G new radio standard from just a theoretical concept with very large number of BS antennas. [3]. The first 64-antenna array equipped and deployed at BS radio by Ericsson AIR, Huawei AAU and Nokia AirScale, called Massive MIMO [3]. This reveals that the Massive MIMO is not just a concept but a reality. There are many papers that have analyzed and well-cited the Massive MIMO technology [3], but most of them have made assumptions as :1) The propagation channels are spatially uncorrelated and 2) The signal processing schemes originally

FOREX Publication
Open Access | Rapid and quality publishing
International Journal of Electrical and Electronics Research (IJEER)
Research Article | Volume 11, Issue 4 | Pages 1001-1012 | e-ISSN: 2347-470X

developed for single-cell operation are applied to multi-cell scenarios by try and error basis. These assumptions are analytically tractable [3], but there are three major gaps: 1) In practice channels are spatially correlated, 2) multi-cell signal processing schemes can provide large gains, and 3) The pilot contamination (PC), also known as inter-cell interference, becomes a potential limiting factor due the simplified assumption above.

There are research articles that have not considered some or all of these gaps [3] and it is fulfilled, but at very slow pace due to the very less tractable analysis. The essential and prominent messages from this direction of research, which contrast and sometime complement the traditional views, are easily ignored since they are minor in the vast literature on Massive MIMO. By the way, this research has explored enough by fundamental works [2-6, 8] and the recent work [5, 6, 8]. That is why our focus in this report particularly on pilot reuse phenomenon and try to summarized that whether pilot reuse is limiting factor or improving factor for SE?

2. LITERATURE REVIEW

The channel correlation, interference suppression and PC at large has been discussed in [3]. Also determined averaged sum SE for various combing and precoding methods for various pilot reuse factors in Rayleigh correlated fading using various channel estimators. The inter-cell coordination scheme, which employ cross-channel covariance matrixes prior information to reuse pilot among well separated UEs, is proposed in [7]. The UE scheduling can improve SE per cell in Massive MIMO network [8]. The pilot overhead can be reduced by pilot reuse concept in single cell in [10]. The pilot overhead is proportional to number of UE antennas in orthogonal training scheme and increase in UE antennas increases pilot overhead extensively and greatly decreases SE. The pilot sequence of UE, closer to BS, can be reused across the multi-cell network and results show improvement over existing pilot reuse method [11]. It is advantageous to coordinates pilot assignment with neighboring cells to avoid first tier interference [12]. The compressive sensing (CS)-based CSI estimation scheme can better mitigate ICI in FDD multi-cell massive MIMO network over single cell with low training overhead [13]. The pilot assignment based on cell sector can improve SE in multi-cell network [14], but it requires covariance matrix estimation in advance and UE grouping scheme, which results in computational complexity. The UE geographical information, power control during training phase, and downlink power control can be used in algorithm of pilot assignment to reduce pilot contamination in [15]. The pilot-based and sub-space-based schemes approached by many authors are reviewed in [16], where sub space offer very less or no overhead with better SE. However, the other schemes can be compared on basis of cost, effectiveness, complexity, processing power, and accuracy. The K-means clustering based pilot allocation algorithm (KCPA) assign pilots to APs and UEs after grouping, which provide effective reduction of PC and as result improve SE [17]. The location-aware pilot assignment is proposed in [18], which uses location of UE to provide CSI. The PC mitigation techniques are reviewed in [19], like orthogonal pilot sequence assignment among adjacent cells, subspace projection-based interference suppression, data-aided channel estimation, and multi-cell cooperation. The arbitrary length pilot sequences are proposed by [20], over existing pilot reuse schemes, having pilot sequence length integer multiple of number UEs. This method increases orthogonality between pilot sequences, mitigate PC and increase SE. The asynchronous pilot transmission (APT) is proposed to improve performance of all UE and fractional pilot reuse (FPR) proposed improve throughput of low-capacity UE in [21]. The graph-based coloring scheme propose in [22], which can well address trade-off between throughput-complexity in cell-free massive MIMO. The max-min sum SE per UE algorithm proposed in [23], which considers pilot assignment and data power control in Massive MIMO with correlated Rayleigh fading scenario and claim as batter than others. The UEs allocation to APs algorithm proposed in [24] for determining initial serving relationships between APs and user UEs and to obtain SE more compared to other algorithm, where adaptive group forming strategy employed for UEs having least common associated APs. The pilot reuse proposed in [25], for single cell in massive MIMO to mitigate pilot overhead and claimed significant gains in SE over the conventional orthogonal training (OT) scheme. As per [26], the BS antennas from 100 to 190 can reduce pilot sequence length requirement from 50 to 25 and UEs can be served with lesser number of pilot reuse factor. This reveals that, the Massive MIMO is key technology for piloting over fast fading channels, where pilot length needs to be short.

3. CORE CONTRIBUTION

For SE enhancement, there are two possible ways, 1) improve pre log factor, which can proportionately increase the SE and 2) improve SINR, which can logarithmically increase the SE, as per SE expression. The pre log factor is ratio of UL/DL data samples to total samples in coherent slot and SINR is ratio of signal power to interference plus noise power. However, using same set of pilots in each cell can reduce required pilot samples in coherent slot, which increases available samples for data transmission in the coherent slot. As result, more bits per second can be transmitted, which reflects as SE enhancement at first look. However, this is one side of whole phenomenon and other side needs to be explored. When same pilot set is used in each cell for channel estimation, UEs with same pilot sequence send their pilot sequence in UL towards their own BS along with other BSs, which creates error in channel estimation, called pilot contamination. As result, inter-cell interference increases, this results in SINR reduction and SE reduction as whole. However, allocating separate pilot set to each cell can remove pilot contamination and inter-cell interference, which looks like SE increases by increasing SINR. However, this is again one side of whole phenomenon and other side needs to be explored. The separate unique pilot set for each cell can increase pilot overhead drastically, which reduces SE by looking from other side. In conclusion, using same pilot set in each cell and using unique pilot set in each cell are two extreme cases. However, not moving towards any of these two extreme cases and reusing pilot set for cluster of cells is the optimum approach, which allows trade-off between Prelog factor and SINR.

FOREX Publication
Open Access | Rapid and quality publishing
International Journal of Electrical and Electronics Research (IJEER)
Research Article | Volume 11, Issue 4 | Pages 1001-1012 | e-ISSN: 2347-470X

As per literature review, very thin lines of papers have approached to determine optimum pilot reuse factor for best SE. Also, most papers have considered uncorrelated fading scenario or Rayleigh fading scenario for channel propagation with in cell or inter-cell. Most research papers have considered single-cell scenario and MIMO or Multi-User MIMO technology have been considered. Also, most research papers have not considered state-of-art channel estimation methods or considered single channel estimation method for research towards optimum pilot reuse factor for best SE. Also, comparison between Bayesian and Non-Bayesian channel estimators for various pilot reuse factors is missing almost in previous research. Above shortfalls are tried to be fulfilled in this article by considering, 1) Correlated Rician channel fading scenario, which is more realistic compared to Rayleigh channel fading, 2) multi-cell network with Massive MIMO technology, 3) Minimum Mean Square Error (MMSE), Element-Wise Minimum Mean Square Error (EW-MMSE), and Least Square Error (LS) channel estimators and 4) Different pilot reuse factors for each channel estimator method for SE performance.

The SE has been determined using above mentioned estimators and different pilot reuse factors by considering multi-cell network with Massive MIMO technology in spatially correlated Rician fading scenario.

4. CHANNEL AND SYSTEM MODELING

This section consists of channel and system modelling with configurations, which are more near to realistic scenario.

4.1 The Basic Cellular Network

In our research work, we have considered Massive MIMO system having hundreds of antennas at BS. Also, the network assumed of L numbers of cells and each cell is assigned with dedicated single BS having M_j number of antennas. In each cell there are K number of UEs, served by dedicated BS within cell. *Figure 1* gives more details view of the same above explanation.

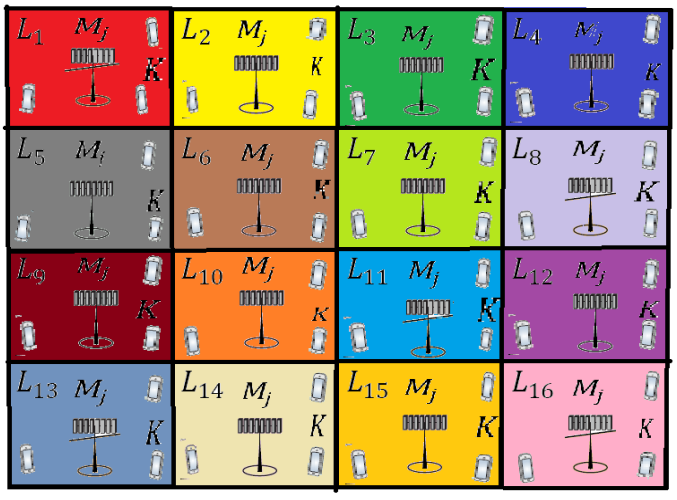

Figure 1: The Massive MIMO Cellular System

4.2 Acquiring Channel State Information

The UL and DL signals are processed on basis of obtained channel responses h_{jk}^{j}. Many a times, it is assumed that the channel responses are know perfectly at BS, which is not the case practically and it needs to be obtained by channel estimation methods. Also, these channel responses are constant for few milliseconds and hundred kHz only. In practice, the channel response changes randomly and it due to that a random distribution is commonly used to model the channel variations.

The set of channel responses for realization is called channel state and BS have knowledge about that is called as channel state information (CSI). The statistical information of random variables distribution is assumed to be available across the network. However, real-time CSI about the real channel realizations need to be acquired at the same pace as the channels change. The piloting is most prominent method for CSI acquisition, where known pilot signals are transmitted in UL from UE. The pilot signal can be received by any other antenna in the network and it can be compared with known pilot signal to estimate channel. However, if we are interested to estimate the channels from two or more separate antennas then two or more orthogonal pilot signals are required and orthogonality can be achieved by employing two or more samples for transmission [2]. The number of orthogonal pilot signals and transmit antennas are proportional to each other. However, any number of receive antennas can simultaneously listen to the pilots and can estimate channels.

The channel responses are reciprocal if UL and DL are separated in time using TDD protocol and channel needs to be estimated in UL only [2].The BS j in cell j estimate channel response h_{jk}^{j} to its kth UE and UE k required to know effective scalar channel $g_k^j = \left(h_{jk}^{j}\right)^H w_{jk}$ which is obtained after precoding. As channels are constant value of g_k^j is constant and it can be obtained from DL data transmission, where channel distribution has no role [2]. The phase of w_{jk} is adjusted according to CSI available at BS. As result, the phase of g_k^j remains almost deterministic and almost only the magnitude $|g_k^j|$ requires to be estimated. The channel hardening can be expressed as $|g_k^j| / \mathbb{E}\{g_k^j\}$ and as this ratio becomes smaller estimation quality gets increased. As a result, only k numbers of pilots are required using a TDD protocol and BS antennas has no role over it.

The channel reciprocity is not present, if UL and DL are separated in frequency using a frequency-division duplex (FDD) protocol. As a result, channel needs to be estimated in both side and pilots needs to be sent in both directions. Also, DL channel estimation needs to be sent back to the BS through UL to prepare DL precoding vectors. So, M + K pilots needs to be sent in UL and M pilots needs to be sent DL in FDD protocol. The FDD protocol needs to provide $\frac{M+K+max\ (M,K)}{2}$ pilot overhead on average in UL/DL, which far greater than TDD.

FOREX Publication
Open Access | Rapid and quality publishing
International Journal of Electrical and Electronics Research (IJEER)
Research Article | Volume 11, Issue 4 | Pages 1001-1012 | e-ISSN: 2347-470X

4.3 Channel Coherence Block

The propagation channels are functions of time and frequency and its change can be analyzed in time and frequency domain. The numbers of complex-valued samples (equals bandwidth B) describe the signal per second. So, bandwidth increase can decrease the time interval between two samples. The signal energy transmitted over time interval is getting spread out and due to that it is received over longer time duration, called dispersive channel. The depressiveness of channel is larger than transmitted sample interval creates extensive overlap between adjacent transmitted samples at receiver. However, it is called channel having memory and it is tuff to estimate channel. Also, it is very hard to process transmitted and received signal due to sever inter-sample interference. The traditional solution is to divide bandwidth into many subcarriers, having smaller bandwidth. This result into longer channel dispersion compared to inter-sample time duration. The information-theoretic concepts can be applied as channel bandwidths are narrower.

Which multi-carrier modulation scheme used is not essential but frequency band getting divided into flat-fading subcarriers important in the context of the Massive MIMO. The channel remains constant over frequency interval is called coherence bandwidth B_c of channel. There are many subcarriers packed into coherent bandwidth, so channel responses observed on adjacent subcarrier are equal or deterministically transformable. This reveals that on every subcarrier channel need not to be estimated. Same way, channel changes are small between adjacent samples. However, time interval over which channel remains constant is called coherent time interval T_c.

A coherence block has two dimensions, coherent bandwidth and coherent time. It is divided into number of subcarriers in coherent bandwidth dimension and divided into number of time samples in coherent time dimensions. Also, channel responses are approximately constant over coherent time and it is flat faded over coherent bandwidth. The number of complex-valued samples in each coherent block are defined as $\tau_c = B_c T_c$.

In coherent block, channel responses are statistically random and identical to the channel response in other coherent block regardless whether they are separated in time and/or frequency. So, channel fading can be modelled as stationary ergodic random process and analysis can be carried out over single coherent block. *Ii* is assumed that the channel can be realized independently over each block, known as block fading. Each coherence block is operational in TDD mode and block samples are used for three different purposes as: 1) τ_p samples for UL piloting 2) τ_u samples for UL data signalling and 3) τ_d samples for DL data signaling, where $\tau_c = \tau_p + \tau_u + \tau_d$ is total samples of coherent block.

The network traffic nature decides the number sample allocation for UL and DL data transmission. However, samples for piloting per coherent block are a design parameter. The video streaming and web browsing are examples, where DL traffic is more compared to UL $(\tau_d > \tau_u)$. The channel coherence block dimensions are decided by the UE mobility, carrier frequency and propagation environment [2]. Each UE has its own coherence bandwidth and time. However, for network it is not possible to adapt for each UE, so practically coherent block size decided for worst case condition that network have to support. The UEs having larger coherence time/bandwidth, can avoid to transmit pilot in each predefined block.

4.4 The Channel Model

The $h_{lk}^j \in \mathbb{C}^{M_j}$ is channel response of propagation, where subscript l, subscript k and superscript j are cell number, equipment number and BS number respectively, which are same throughout the article. Each element of channel response vector represents propagation of signal from user equipment to any one of M_j antennas of BS. For notational convenience, h_{lk}^j is used for UL channel and $\left(h_{lk}^j\right)^H$ used for DL channel, since there is no difference in channel response in UL and DL in same coherent slot.

In general, the channel can be modelled as,

$$h_{lk}^j \sim \mathcal{N}_{\mathbb{C}}\left(\bar{h}_{lk}^j, R_{lk}^j\right), \quad (1)$$

Where $\forall j, l \in 1, \ldots, L$ and $\forall k \in 1, \ldots K$ and channel realization assumed as the circularly symmetric complex Gaussian distribution. In equation (1), the channel mean $\bar{\mathrm{h}}_{lk}^j \in \mathbb{C}^{M_j}$ represents the LoS component and positive semi-definite covariance matrix $R_{lk}^j \in \mathbb{C}^{M_j \times M_j}$ represents to NLoS components with spatial correlation. The Gaussian distribution describes small-scale fading and macroscopic propagation effects represent the radiation patterns of antennas, path loss, and shadow fading, which can be modeled by R_{lk}^j and $\bar{\mathrm{h}}_{lk}^j$.

5. CHANNEL ESTIMATION

This section is dedicated to understand channel estimation process and methods

5.1 Up-link Pilot Transmission

Each BS needs to estimate channels from active UEs within coherent block to make efficient usage of Massive MIMO. The BS should have channel estimates from its own UEs. Also, the channel estimates from interfering UEs in other cells are also as essential as channel estimates from its own UEs to mitigate inter-cell interference. The pilot signal transmitted by τ_P samples. The pilot sequence of UE k in cell j is denoted by $\emptyset_{jk} \in \mathbb{C}^{\tau_P}$, where $\left\|\emptyset_{jk}\right\|^2 = \emptyset_{jk}^H \emptyset_{jk} = \tau_P$. The elements of UL pilot $\emptyset_{jk}$ vector are multiplied by the UL transmit power $\sqrt{P_{jk}}$ and it is transmitted as signal s_{jk} using τ_P UL samples, which results in received UL signal $Y_j^p \in \mathbb{C}^{M_j \times \tau_P}$ at BS j as shown below,

$$Y_j^p = \sum_{k=1}^{K_j} \sqrt{P_{jk}}\, h_{jk}^j \emptyset_{jk}^T + \sum_{\substack{l=1 \\ l \neq j}}^{L} \sum_{i=1}^{K_l} \sqrt{P_{li}}\, h_{li}^j \emptyset_{li}^T + N_j^p \quad (2)$$

Where $N_j^p \epsilon\, \mathbb{C}^{M_j \times \tau_P}$ is independent additive receiver noise with $\mathcal{N}_{\mathbb{C}}\,(0, \sigma_{UL}^2)$. Now for example, if BS j wants to estimate channel

FOREX Publication
Open Access | Rapid and quality publishing
International Journal of Electrical and Electronics Research (IJEER)
Research Article | Volume 11, Issue 4 | Pages 1001-1012 | e-ISSN: 2347-470X

h_{li}^{j} from an arbitrary UE *i* in cell *l* then BS needs to multiply Y_j^p with pilot sequence $\emptyset_{li}$ of UE *i* in cell *l* , results into the processed received pilot signal $y_{jli}^p \in \mathbb{C}^{M_j}$, given as

$$y_{jli}^p = Y_j^p \emptyset_{li}^* = \sum_{l'=1}^{L} \sum_{i'=1}^{K_{l'}} \sqrt{P_{l'i'}} h_{l'i'}^{j} \emptyset_{l'i'}^T \emptyset_{li}^* + N_j^p \emptyset_{li}^* \quad (3)$$

Equation (3) can be rewrite for UE *k* in its own BS *j* as,

$$y_{jjk}^p = Y_j^p \emptyset_{jk}^* = \sqrt{P_{jk}} h_{jk}^{j} \emptyset_{jk}^T \emptyset_{jk}^* + \sum_{\substack{i=1 \\ i \neq k}}^{K_j} \sqrt{P_{ji}} h_{ji}^{j} \emptyset_{ji}^T \emptyset_{jk}^* + \sum_{\substack{l=1 \\ l \neq j}}^{L} \sum_{i=1}^{K_l} \sqrt{P_{li}} h_{li}^{j} \emptyset_{li}^T \emptyset_{jk}^* + N_j^p \emptyset_{jk}^* \quad (4)$$

In *equation (4)*, second and third terms are signifying interference. Also, they contain inner product of pilots $\emptyset_{li}^T \emptyset_{jk}^*$ of the desired UE and of another UE *i* in cell *l*. The interference term is zero if pilot sequences are orthogonal and estimation does not contaminate. It is expected that, all pilot sequences are orthogonal, but due to limited length τ_P of pilot sequence only τ_P mutually orthogonal sequences are possible. However, coherent block length is finite and as a result $\tau_P \leq \tau_c$, which indicates that it is not possible to assign mutually orthogonal pilots to all UEs in practice. Also, for longer pilots, it needs to compromise with fewer samples for data transmission. Usually, τ_P should always be smaller than $\tau_c/2$ [2].

The UL pilot book can be defined as $\Phi \in C^{\tau_P \times \tau_P}$, where $\Phi^H \Phi = \tau_P I_{\tau_P}$. It is expected to have $\tau_P \geq max_l K_l$ pilots to allocate separate pilot sequence to each UE, otherwise severe interference from within a cell is possible. The set can be defined as below,

$$\mathcal{P}_{jk} = \{(l,i) : \emptyset_{li} = \emptyset_{jk}, l = 1, \dots, L, i = 1, \dots, K_l\} \quad (5)$$

for all UEs that utilize the same pilot sequence as UE *k* in cell *j*. In other words, $(l,i) \in \mathcal{P}_{jk}$, means UE *i* in cell *l* uses the same pilot as UE *k* in cell *j*.

Equation (4) can be simplified as below using notation in *equation (5)*,

$$y_{jjk}^p = \sqrt{P_{jk}} \tau_P h_{jk}^{j} + \sum_{(l,i) \in \mathcal{P}_{jk} \setminus (j,k)} \sqrt{P_{li}} \tau_P h_{li}^{j} + N_j^p \emptyset_{jk}^* \quad (6)$$

Note that $y_{jjk}^p = y_{jli}^p$ for all $(l,i) \in \mathcal{P}_{jk}$, since these UEs use the same pilot. We also note that $N_j^p \emptyset_{jk}^* \sim \mathcal{N}_{\mathbb{C}}\left(0, \sigma_{UL}^2 \tau_P I_{M_j}\right)$, since the pilot sequences are deterministic and $\|\emptyset_{jk}\|^2 = \tau_P$.

In *equation (6)*, y_{jjk}^p is sufficient statistic for estimating h_{jk}^{j} without loss of information, instead of using original received signal Y_j^p [2]. Because, by multiplying y_{jjk}^p with $\emptyset_{jk}^T$ can brought back $h_{jk}^{j} \emptyset_{jk}^T$ in Y_j^p and interference terms become zero or brought back.

5.2 Channel Estimation Methods

The channel estimator can be derived from the channel response h_{li}^{j}, using Y_j^p in *equation (2)* and a pilot book. The Bayesian estimators are suitable for channel estimation, since channels are realization of random variables and its statistical distribution is accounted [2]. Bayesian estimators needs channel distributions known.

5.3 MMSE Channel Estimator

The minimum mean-squared error (MMSE) estimator of h_{li}^{j} is defined as $\hat{h}_{li}^{j}$, which minimizes the MSE $\mathbb{E}\left\{\left\|h_{li}^{j} - \hat{h}_{li}^{j}\right\|^2\right\}$. The received pilot signal as per *equation (2)* can be processed using MMSE channel estimator as per below,

$$\hat{h}_{li}^{j} = \bar{h}_{li}^{j} + \sqrt{P_{li}} R_{li}^{j} \Psi_{li}^{j} \left(y_{jli}^p - \bar{y}_{jli}^p\right) \quad (7)$$

where $\hat{h}_{li}^{j}$ is channel estimation, $\bar{h}_{li}^{j}$ is channel mean, y_{jli}^p is processed received pilot signal, and $\bar{y}_{jli}^p = \sum_{(l',i') \in p_{li}} \sqrt{P_{l'i'}} \tau_P \bar{R}_{l'i'}^{j}$ is processed received pilot signal mean. Inverse of $\frac{\left\{y_{jli}^p y_{jli}^{p\,H}\right\}}{\tau_p}$ is defined as h_{li}^{j} and it can be expressed as,

$$\Psi_{li}^{j} = \tau_P Cov\left\{y_{jli}^p\right\}^{-1} = \left(\sum_{(l',i') \in p_{li}} P_{l'i'} \tau_P R_{l'i'}^{j} + \sigma^2 I_{M_j}\right)^{-1} \quad (8)$$

It is noticeable here that, fully known statistical distribution required by Bayesian MMSE estimator. The estimation error $\tilde{h}_{li}^{j} = h_{li}^{j} - \hat{h}_{li}^{j}$ covariance matrix can be expressed as,

$$C_{li}^{j} = \mathbb{E}\left\{\tilde{h}_{li}^{j} \left(\tilde{h}_{li}^{j}\right)^H\right\} = R_{li}^{j} - P_{li} \tau_P R_{li}^{j} \Psi_{li}^{j} R_{li}^{j} \quad (9)$$

The channel estimation of channel h_{li}^{j} in *equation (6)* required to correlate y_{jli}^p with Y_j^p at BS. After that, it needs to multiply with Ψ_{li}^{j} and R_{li}^{j} matrices, which mitigate interference and noise having no second-order statistics like h_{li}^{j}. However, it is noticeable that the MMSE estimator $\hat{h}_{li}^{j}$ is linear.

The MMSE estimate h_{li}^{j} and estimation error $\hat{h}_{li}^{j}$ are expressed as below,

$$\hat{h}_{li,MMSE}^{j} \sim \mathcal{N}_{\mathbb{C}}\left(\bar{h}_{li}^{j}, R_{li}^{j} - C_{li}^{j}\right), \quad (10)$$

$$\tilde{h}_{li,MMSE}^{j} \sim \mathcal{N}_{\mathbb{C}}\left(0_M, C_{li}^{j}\right) \quad (11)$$

The $\hat{h}_{li}^{j}$ and $\tilde{h}_{li}^{j}$ are independent random variables. Note that the mean value does not have any effect on estimation error covariance matrix C_{li}^{j}. In other way, LoS component do not affect the estimation error as they are known and can be removed from the received signals [9]. However, if $\hat{h}_{jk}^{j}$ and $\hat{h}_{li}^{j}$ utilizing same pilot sequences as $\emptyset_{li} = \emptyset_{jk}$, then $\Psi_{jk}^{j} = \Psi_{li}^{j}$ and $y_{jjk}^p = y_{jli}^p$ .Only R_{jk}^{j} and R_{li}^{j} can differ in correlated fading. This phenomenon is called pilot contamination.

FOREX Publication
Open Access | Rapid and quality publishing
International Journal of Electrical and Electronics Research (IJEER)
Research Article | Volume 11, Issue 4 | Pages 1001-1012 | e-ISSN: 2347-470X

However, $R_{jk}^{j} = \beta_{jk}^{j} I_{M_j} = R_{li}^{j} I_{M_j}$ for uncorrelated fading case and channel estimates are scaled version of each other. This is special case, when BS is not able to separate out channel estimates of UEs having same pilot sequence and spatial characteristics.

5.4 Element Wise MMSE Channel Estimator

If there is computational complexity constraint at BS, then alternative is EW-MMSE, where diagonal element of h_{li}^{j} are estimated and off diagonal elements are left without estimation. As a result, EW-MMSE is simplex more in terms of computational intensity as compared to MMSE, since matrix inversions are not required. The channel estimation by EW-MMSE is defined as,

$$\hat{h}_{li}^{j} = \bar{h}_{li}^{j} + \sqrt{P_{li}} D_{li}^{j} \Lambda_{li}^{j} (y_{jli}^{p} - \bar{y}_{jli}^{p}) \quad (12)$$

Where $D_{li}^{j} \in \mathbb{C}^{M_j \times M_j}$ and $\Lambda_{li}^{j} \in \mathbb{C}^{M_j \times M_j}$ are diagonal matrices and expressed as,

$$D_{li}^{j} = diag\left(\left[R_{li}^{j} \right]_{mm} : m = 1 \dots M_j \right) \quad (13)$$

$$\Lambda_{li}^{j} = diag\left(\left[\sum_{(l',i') \in p_{li}} P_{l'i'} \tau_P R_{l'i'}^{j} + \sigma^2 I_{M_j} \right]_{mm} : m = 1 \dots M_j \right)^{-1} \quad (14)$$

The EW-MMSE estimation $\hat{h}_{li}^{j}$ and estimation error $\tilde{h}_{li}^{j}$ can be distributed as below and they are correlated random variables,

$$\hat{h}_{li,EW-MMSE}^{j} \sim \mathcal{N}_{\mathbb{C}} \left(\bar{h}_{li}^{j}, \Sigma_{li}^{j} \right) \quad (15)$$

$$\tilde{h}_{li,EW-MMSE}^{j} \sim \mathcal{N}_{\mathbb{C}} \left(0_M, \tilde{\Sigma}_{li}^{j} \right) \quad (16)$$

where Σ_{li}^{j} and $\tilde{\Sigma}_{li}^{j}$ can be expressed as below,

$$\Sigma_{li}^{j} = P_{li} \tau_p D_{li}^{j} \Lambda_{li}^{j} (\Psi_{li}^{j})^{-1} \Lambda_{li}^{j} D_{li}^{j} \quad (17)$$

$$\tilde{\Sigma}_{li}^{j} = P_{li} \tau_p R_{li}^{j} \Lambda_{li}^{j} D_{li}^{j} - P_{li} \tau_p D_{li}^{j} \Lambda_{li}^{j} R_{li}^{j} + \Sigma_{li}^{j} \quad (18)$$

It is noticeable that if covariance matrices have none zero diagonal elements and zero off diagonal elements then there is same performance result of EW-MMSE as it can be with MMSE. In such cases EW-MMSE estimation is optimal choice, as less computational efforts required than MMSE estimation.

5.5 LS Channel Estimator

However, if diagonal elements of channel matrix are not possible to be estimated by anyhow (due to rapid change in channel), then third and least option is least-square (LS) channel estimation. The LS does not require any prior channel estimation statistics and it is used since start of SDMA [9]. The LS estimate $\hat{h}_{li}^{j}$ can be defined as vector, which minimize $\left\| y_{jli}^{p} - \sqrt{P_{li}} \tau_P \hat{h}_{li}^{j} \right\|^2$. The perfect LS estimate can be defined as,

$$\hat{h}_{li}^{j} = \frac{1}{\sqrt{P_{li}} \tau_P} y_{jli}^{p} \quad (19)$$

where $\hat{h}_{li}^{j}$ and $\tilde{h}_{li}^{j}$ are estimation and estimation error of channel respectively and their distributions are expressed as,

$$\hat{h}_{li,LS}^{j} = \mathcal{N}_{\mathbb{C}} \left(\frac{1}{\sqrt{P_{li}} \tau_P} \bar{y}_{jli}^{p}, \frac{1}{P_{li} \tau_P} \Psi_{li}^{j-1} \right) \quad (20)$$

$$\tilde{h}_{li,LS}^{j} = \mathcal{N}_{\mathbb{C}} \left(\bar{h}_{li}^{j} - \frac{1}{\sqrt{P_{li}} \tau_P} \bar{y}_{jli}^{p}, \frac{1}{P_{li} \tau_P} \Psi_{li}^{j-1} - R_{li}^{j} \right) \quad (21)$$

respectively. The $\hat{h}_{li}^{j}$ and $\tilde{h}_{li}^{j}$ are correlated random variables.As it is noticeable, LS channel estimation is computationally simple than other two methods, but LS estimation has to pay for that by having channel estimation statistics more complex than other two estimators. This can be seen in above *equation (21)* as non-zero mean in estimation error and it is compromise in communication performance.

6. UP-LINK & DOWN LINK SPECTRAL EFFICIENCY

This section is dedicated to UL and DL SEs analysis using channel estimators discussed in previous section. The UE k in cell j transmits a random data signal $s_{jk} \sim \mathcal{N}_{\mathbb{C}}(0, p_{jk})$ for j = 1, . . ., L and k = 1, . . ., K_j. The p_{jk} is transmit power per sample. The received signal $y_j \in \mathbb{C}^{M_j}$ at BS j, during data transmission, is,

$$y_j = \sum_{k=1}^{K_j} h_{jk}^{j} s_{jk} + \sum_{\substack{l=1 \\ l \neq j}}^{L} \sum_{i=1}^{K_l} h_{li}^{j} s_{li} + n_j \quad (22)$$

where n_j is additive noise with distribution $n_j \sim \left(0_{M_j}, \sigma^2 I_{M_j} \right)$. In *equation (22)* first term is desired signal; second term is interference and last term is noise.

The $v_{jk} \in \mathbb{C}^{M_j}$ is combing vector selected by BS j for its UE k and it is derived from obtained channel estimates. It also depends on channel estimates of other UEs to mitigate interference from other UEs. The received signal y_j is correlated with combing vector ${v_{jk}}^H$ as per below,

$${v_{jk}}^H y_j = {v_{jk}}^H \hat{h}_{jk}^{j} s_{jk} + {v_{jk}}^H \tilde{h}_{jk}^{j} s_{jk} + \sum_{\substack{i=1 \\ i \neq k}}^{K_j} {v_{jk}}^H h_{ji}^{j} s_{ji} + \sum_{\substack{l=1 \\ l \neq j}}^{L} \sum_{i=1}^{K_l} {v_{jk}}^H h_{li}^{j} s_{li} + {v_{jk}}^H n_j \quad (23)$$

In *equation (23)*, first term is desired signal over estimated channel, second term is desired signal over unknown channel, third term is Intra-cell interference, fourth term is inter-cell interference and last term is noise. The first term is totally for signal detection, while the second term is for estimation error vector distribution knowledge. The letter term considered additional interference for signal detection.

The UL ergodic channel capacity of UE k in cell j is lower bounded by SE_{jk}^{ul} [bit/s/Hz] and it can be expressed as [2],

$$SE_{jk}^{ul} = \frac{\tau_u}{\tau_c} \log_2 (1 + \gamma_{jk}^{ul}) \text{ bits/s/Hz} \quad (24)$$

where γ_{jk}^{ul} is effective SINR expressed as,

FOREX Publication
Open Access | Rapid and quality publishing
International Journal of Electrical and Electronics Research (IJEER)
Research Article | Volume 11, Issue 4 | Pages 1001-1012 | e-ISSN: 2347-470X

$$\gamma_{jk}^{ul} = \frac{p_{jk}\left|\mathbb{E}\{v_{jk}^H h_{jk}^j\}\right|^2}{\sum_{l=1}^{L}\sum_{i=1}^{K_l} p_{li}\mathbb{E}\left\{\left|v_{jk}^H h_{li}^j\right|^2\right\} - p_{jk}\left|\mathbb{E}\{v_{jk}^H h_{jk}^j\}\right|^2 + \sigma_{ul}^2\mathbb{E}\{\|v_{jk}\|^2\}} \quad (25)$$

where expectation is carried out from all sources of randomness.

The pre-log factor $\frac{\tau_u}{\tau_c}$ in (24) is the fraction of samples per coherence block that are used for UL data. Since $\tau_u = \tau_c - \tau_p - \tau_d$, the pre-log factor can be increased by shorting τ_p samples and/or shorting samples τ_d. The SE expression provided in *equations (24)* is true for any receive combining method. However, the MR combining $(v_{jk} = \hat{h}_{jk}^j)$ is generally used in the Massive MIMO and it is also considered here in our configuration. However, for MMSE and EW-MMSE estimators the MR combing vector is $v_{jk} = \hat{h}_{jk}^j$ in UL, and for LS estimator the MR combing vector is $v_{jk} = \frac{1}{\sqrt{p_{jk}\tau_p}} y_{jjk}^p$.

The reverse process can be followed for Down-Link (DL) spectral efficiency measurement. In which, data signal is transmitted from BS and received at UE. Here it is noticeable that the channel is estimated only in UL and considered same in downlink as per TTD protocol. The closed form equations of DL SE and SINR can be derived as like UL and followed for analysis. The DL SE SE_{jk}^{dl} and SINR γ_{jk}^{dl} can be achieved using MR pre-coding, where for MMSE, EW-MMSE and LS estimators the MR pre-coding vector is $w_{lk} = \frac{\hat{h}_{jk}^j}{\sqrt{\mathbb{E}\left\{\left\|\hat{h}_{jk}^j\right\|^2\right\}}}$. In this section, the different receive combining schemes are evaluated, and the impacts of spatial channel correlation and pilot contamination are revisited.

7. DESIGN AND SIMULATION METHODOLOGY

This section describes design parameters and simulation method with flow-chart.

7.1 Design Parameters

Total 16 cells network configured, where each cell shape considered square with area 250m x 250m. The wrap around topology considered for cellular network, which ensure substantially equal interference to each BS from every direction. The *table 1* provides basic system parameters and its values used in our experimental setup.

Table 1: System Parameters and Its Values for Experiment Set-Up. [2], [9]

Network layout	Square pattern with grid of 4 x 4 cells (Wrap-Around Topology)
Number of Cells	16
Cell Area	0.25 km x 0.25 km
Number of antennas per BS	M =100
Number of UEs per cell	K = 10, distributed uniformly and independently at least 35 m away from BS
Channel gain at 1 km	$\Upsilon = -148.1$ dB
Pathloss exponent	$\alpha = 3.76$
Shadow fading (standard deviation)	$\sigma sf = 10$
Bandwidth	B = 20MHz
Receiver noise power	−94dBm
UL transmit power	20dBm
DL transmit power	20dBm
Samples per coherence block	$\tau c = 200$
Pilot reuse factor	f = 1,2,4,8, and 16
Number of UL pilot sequences	$\tau p = fK$

There are 10 UEs per cell considered, which are served by 100 BS antennas. The UEs are distributed independently and uniformly in each cell at least 35m away from BS. The UE assignment to the single BS among possible BSs options is carried out by ensuring largest channel gain availability to that BS. The large scale fading and nominal angle are computed from UE locations. The uniformly half wave-length spaced and linearly distributed (ULA) antennas are considered at each BS. The number of scattering clusters N is considered 6 [27] for covariance matrices and it is approximately modeled as,

$$\left[R_{li}^j\right]_{s,m} = \frac{\beta_{li}^{j,NLoS}}{N}\sum_{n=1}^{N} e^{j\pi(s-m)\sin(\varphi_{li,n}^j)} e^{-\frac{\sigma_\varphi^2}{2}\left(\pi(s-m)\cos(\varphi_{li,n}^j)\right)^2} \quad (26)$$

where $\beta_{lk}^{j,NLoS}$ is the large scale fading co-efficient for non direct paths and $\varphi_{li,n}^j \sim \mathcal{U}\left[\varphi_{li}^j - 40^o, \varphi_{li}^j + 40^o\right]$ is the nominal angle of arrival [9], where n is the number of clusters, s is row number and m is column number of R_{li}^j. The Gaussian local scattering model [2] is considered for the covariance matrix $\left[R_{li}^j\right]_{s,m}$ of each cluster. The Gaussian distributed Angle of Arrivals (AoAs) of multipath components of a cluster, is distributed with the Angular Standard Deviation (ASD) $\sigma_\varphi = 5^o$ around the nominal AoA [2]. The channel bandwidth for communication is 20 MHz and the total receive noise power is -94 dBm considered [2]. The number of samples per coherent slot is considered 200. Each UE in the cell is assigned unique pilot sequence randomly. However, pilot reuse factor considered 1, 2, 4, 8, and 16. It is possible that the UEs of different cells are assigned with same pilot sequence except pilot reuse factor 16 in 16 cells network.

There are always dominant LoS paths available between UE and BS pairs and the large-scale fading coefficient in presence of LoS paths, is modeled (in dB) as [27]

$$\beta_{li}^j = -30.18 - 26\log_{10}\left(d_{li}^j\right) + F_{li}^j \quad (27)$$

Where shadow fading is $F_{li}^j \sim \mathcal{N}(0, \sigma_{sf}^2)$ with $\sigma_{sf} = 4$ [27]. The formula for Rician factor is $k_{li}^j = 13 - 0.03d_{li}^j$ [dB] [27]. The large scale fading parameters in terms of large scale fading coefficient β_{li}^j and Rician factor k_{li}^j are defined as [27]

FOREX Publication
Open Access | Rapid and quality publishing
International Journal of Electrical and Electronics Research (IJEER)
Research Article | Volume 11, Issue 4 | Pages 1001-1012 | e-ISSN: 2347-470X

$$\beta_{li}^{j,LoS} = \sqrt{\frac{k_{li}^{j}}{k_{li}^{j}+1}}\beta_{li}^{j} \text{ and } \beta_{li}^{j,NLoS} = \sqrt{\frac{1}{k_{li}^{j}+1}}\beta_{li}^{j} \quad (28)$$

For optimum power allocation, the UL power control policy decided by heuristic approach as [2]

$$p_{jk} = \begin{cases} p_{max}^{ul}, & ,\Delta > \frac{\beta_{jk}^{j}}{\beta_{j,min}^{j}}, \\ p_{max}^{ul}\Delta\frac{\beta_{j,min}^{j}}{\beta_{jk}^{j}}, & \Delta \leq \frac{\beta_{jk}^{j}}{\beta_{j,min}^{j}}, \end{cases} \quad (29)$$

where p_{jk} is the transmit power. The p_{max}^{ul} is maximum UL power with value 10 dBm and minimum large scale fading coefficient defined as $\beta_{j,min}^{j} = \min(\beta_{j1}^{j}, \ldots \beta_{jk}^{j} \ldots, \beta_{jK}^{j})$. The policy allows the weakest channel user equipment with full power and reduces power of the remaining UEs such that their UL SNRs are not more than $\Delta = 10\ dB$ higher. The power received by UE ρ_{jk} considered same as power transmitted by US p_{jk} for simplicity. So, above *equation (29)* can be applicable for DL SE measurement also, with just notational change.

7.2 Simulation Set-Up and Pilot Reuse Factor

This section illustrates basic simulation set-up and pictorial view of pilot reuse concept with examples for f = 1, f=2, f = 4, f = 8, and f = 16.

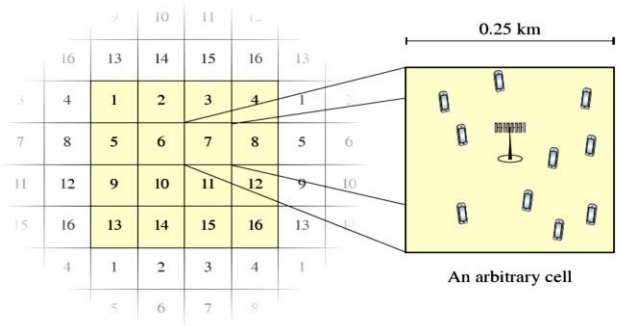

Figure 2: Basic Simulation Set-up

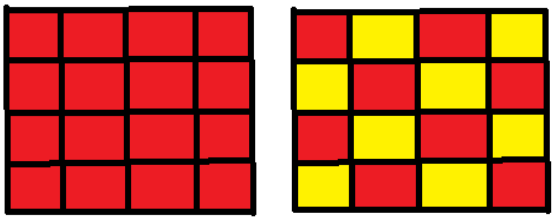

f = 1 f = 2

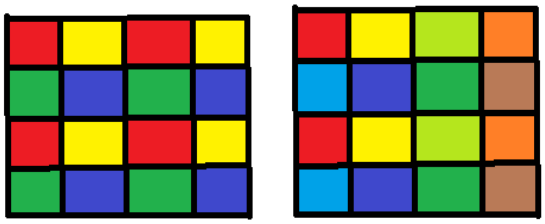

f = 4 f = 8

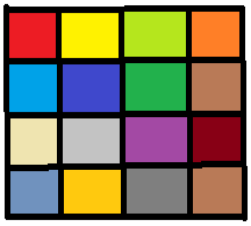

f = 16

Figure 3: Pilot Reuse Factor Pictorial View

Figure 3 illustrate detailed pictorial view of pilot reuse concept. In figure, a different color indicates different pilot sets and a same color indicates same pilot sets. There are five examples has been given for pilot reuse factor 1, 2, 4, 8, and 16. Here it can be seen that the same pilot set-cells are far away from each other as much as possible.

7.3 Simulation and Flow Chart

The MATLAB® simulation software has been used for our analysis. Also, for better explanation of simulation flow below find flow-chart.

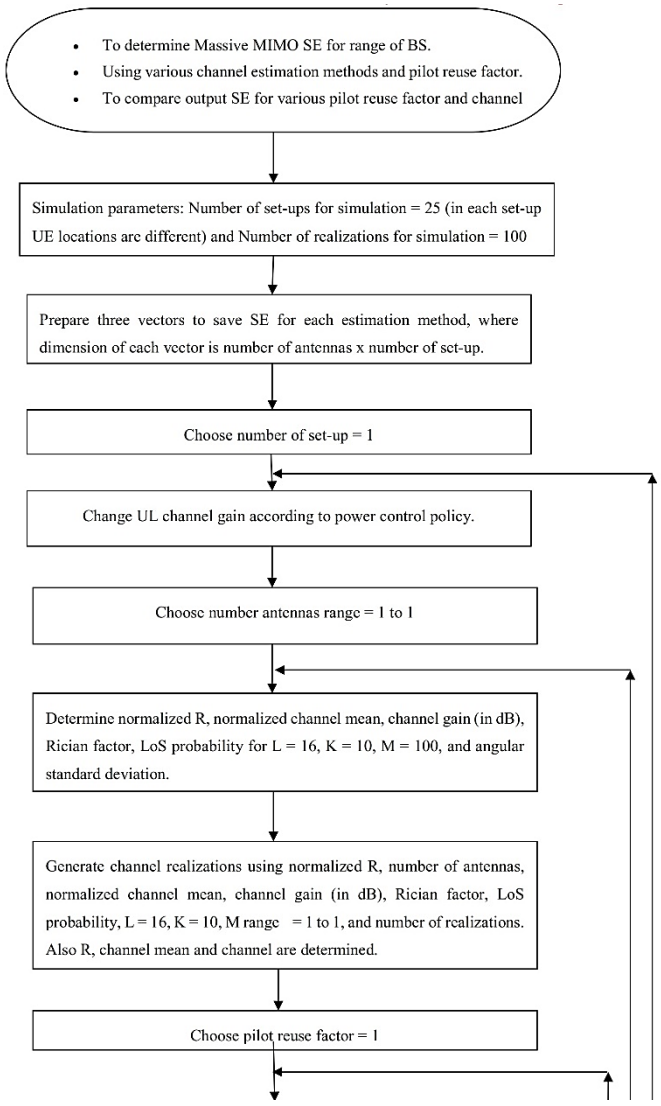

FOREX Publication
Open Access | Rapid and quality publishing
International Journal of Electrical and Electronics Research (IJEER)
Research Article | Volume 11, Issue 4 | Pages 1001-1012 | e-ISSN: 2347-470X

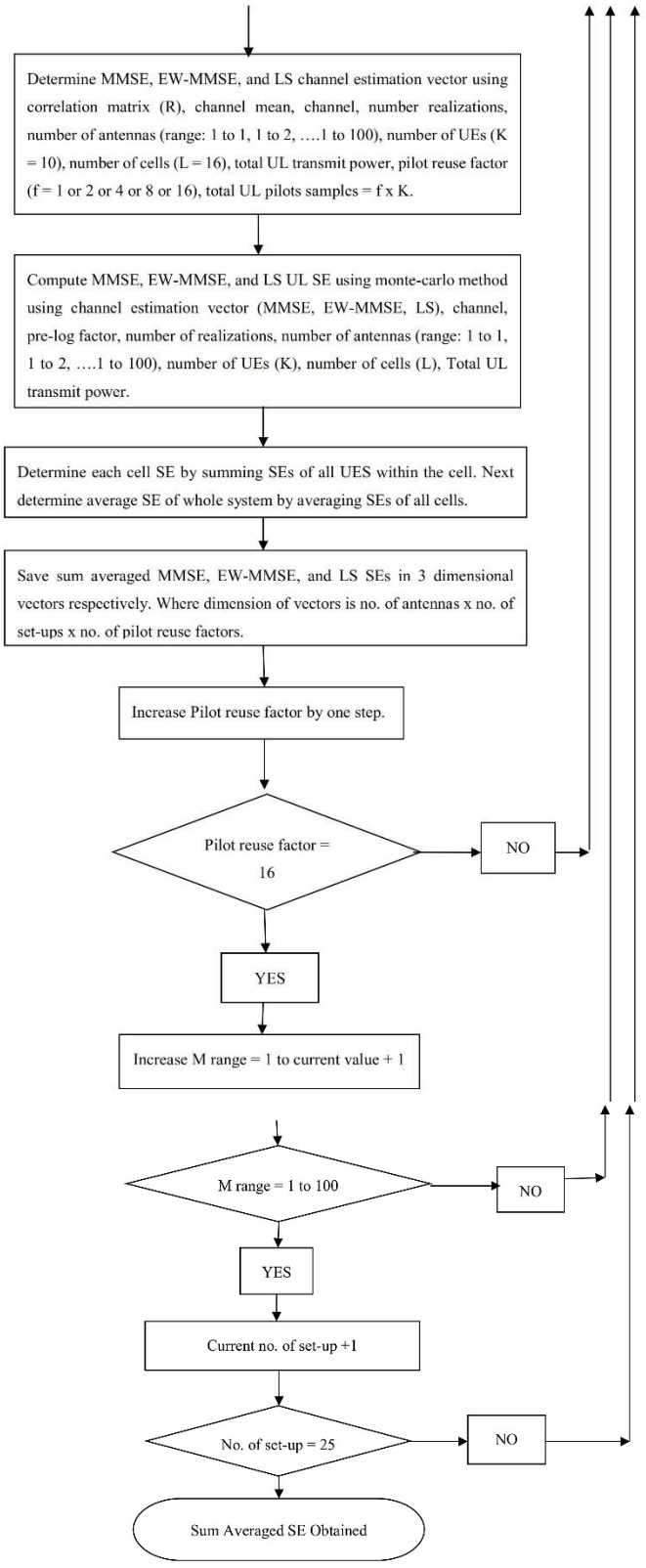

Figure 4: Basic Methodology in Flow-Chart

8. OUTPUT RESULTS

In this section, SE have been carried out for various pilot reuse factors using three estimation methods MMSE, EW-MMSE and LS using MATLAB® simulation.

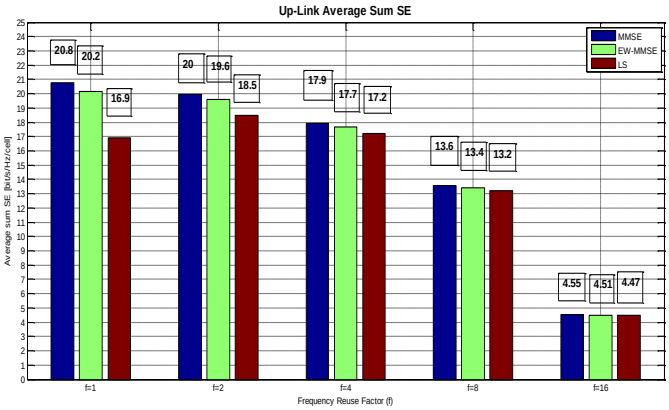

Figure 5: Average Sum UL SE vs. Pilot Reuse Factor for Different Estimation Methods

The *figure 5* provides plots of average sum UL SE for different pilot reuse factors using MMSE, EW-MMSE and LS estimation methods over number of realizations of various shadow fading and user equipment locations. Also, the MR combing method has been chosen for receive combing. The bunch of three bar graphs has been plotted for each pilot reuse factor. In each bunch of graphs blue, green and magenta color bar indicates SE for MMSE, EW-MMSE and LS estimation methods respectively. The value in each box above each bar graph indicates SE of that bar graph. As seen from *figure 5*, as pilot reuse factor increases pre-log factor in SE expression at *equation (24)* decreases and SINR in (*equations 24 & 25*) increases. As result, in SE expression at (24), pre-log factor decrement, which is outside the logarithmic function in *equation (24)*, dominates the increment of SINR in *equations (24)*, which inside the logarithmic function in *equation (24)*. So overall, with increasing pilot reuse factor, SE is decreasing slowly up to pilot reuse factor 4 as seen in *figure 5*. However, it can be clearly visible that the performance of MMSE, EW-MMSE and LS estimators is in descending order respectively for pilot reuse factor 1 as seen from *figure 5*. Also, the performance gap between these estimators is decreasing with increase in pilot reuse factor, because as pilot reuse factor increases inter-cell interference due to pilot contamination decreases. However, the MMSE, EW-MMSE and LS estimators can combat inter-cell interference better in descending order. So, in case, the inter-cell interference due to pilot contamination decreasing, the performance of MMSE, EW-MMSE and LS estimators are going to be closer as can be seen from *figure 5*. In line with that, the performance of three estimators is almost equal for pilot reuse factor 8 and 16, but SE achieved for same pilot reuse factors are lower compared to other lower pilot reuse factors. In conclusion, the SE has been decreased 13.94 %, 12.37 % and 7.03 % for MMSE, EW-MMSE and LS estimators respectively at pilot reuse factor 4 from its maximum value at pilot reuse factor 1 or 2, which is nominal. On the other hand, the performance gap in terms of maximum SE value to minimum SE value of estimators has

FOREX Publication
Open Access | Rapid and quality publishing
International Journal of Electrical and Electronics Research (IJEER)
Research Article | Volume 11, Issue 4 | Pages 1001-1012 | e-ISSN: 2347-470X

been decreased 18.75% to 7.50% to 3.91% respectively for pilot reuse factor 1 to 2 to 4, which is noteworthy.

In conclusion, it is possible to achieve same SE using lower computational complexity estimator compared to higher computational complexity estimator with use of optimum pilot reuse factor.

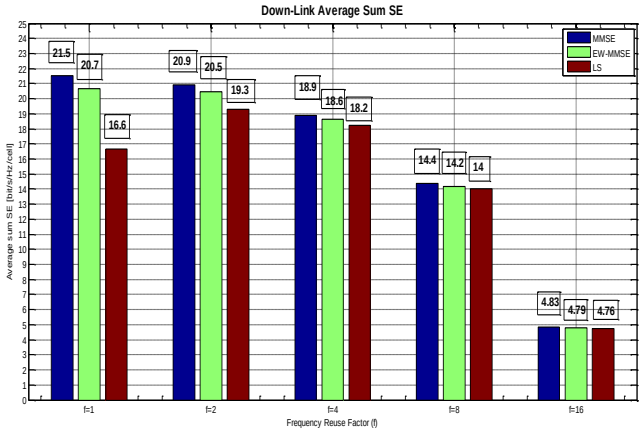

Figure 6: Average Sum DL SE vs. Pilot Reuse Factor for Different Estimation Methods

The *figure 6* provides plots of average sum DL SE for different pilot reuse factors using MMSE, EW-MMSE and LS estimation methods over number of realizations of various shadow fading and user equipment locations. Also, the MR combing method has been chosen for receive combing. The bunch of three bar graphs has been plotted for each pilot reuse factor. In each bunch of graphs blue, green and magenta color bar indicates SE for MMSE, EW-MMSE and LS estimation methods respectively. The value in each box above each bar graph indicates SE of that bar graph. As seen from *figure: 6*, as pilot reuse factor increases, pre-log factor in SE expression at (24) decreases and SINR in (*equations 24 & 25*) increases. However, note that *equation (24) and (25)* can be applicable to for DL SE also with required notational changes. As result, in SE expression at *equations (24)*, pre-log factor decrement, which is outside the logarithmic function in *equation (24)*, dominates the increment of SINR in *equation (24)*, which inside the logarithmic function in *equation (24)*. So overall, with increasing pilot reuse factor, SE is decreasing slowly up to pilot reuse factor 4 as seen in *figure 6*. However, it can be clearly visible that the performance of MMSE, EW-MMSE and LS estimators is in descending order respectively for pilot reuse factor 1 as seen from *figure 6*. Also, the performance gap between these estimators is decreasing with increase in pilot reuse factor, because as pilot reuse factor increases inter-cell interference due to pilot contamination decreases. However, the MMSE, EW-MMSE and LS estimators can combat inter-cell interference better in descending order. So, in case, the inter-cell interference due to pilot contamination decreasing, the performance of MMSE, EW-MMSE and LS estimators are going to be closer as can be seen from *figure 6*. In line with that, the performance of three estimators is almost equal for pilot reuse factor 8 and 16, but SE achieved for same pilot reuse factors are lower compared to other lower pilot reuse factors. In conclusion, the SE has been decreased 12.09 %, 10.14 % and 5.70 % for MMSE, EW-MMSE and LS estimators respectively at pilot reuse factor 4 from its maximum value at pilot reuse factor 1 or 2, which is nominal. On the other hand, the performance gap in terms of maximum SE value to minimum SE value of estimators has been decreased 22.79 % to 7.66 % to 3.70 % respectively for pilot reuse factor 1 to 2 to 4, which is noteworthy.

Table 2: Comparison of Output Results

Estimation Method	UL-SE (bits per second per Hz) for Pilot Reuse Factor					DL-SE (bits per second per Hz) for Pilot Reuse Factor				
	1	2	3	4	5	1	2	3	4	5
MMSE	20.8	20	17.9	13.6	4.55	21.5	20.9	18.9	14.4	4.83
EW-MMSE	20.2	19.6	17.7	13.4	4.51	20.7	20.5	18.6	14.2	4.79
LS	16.9	18.5	17.2	13.2	4.47	16.6	19.3	18.2	14	4.76

In conclusion, it is possible to achieve same SE using lower computational complexity estimator compared to higher computational complexity estimator with use of optimum pilot reuse factor. Find *table 2* for comparative analysis of SE for various pilot reuse factors and channel estimation methods.

9. CONCLUSION

The Massive MIMO provides attractive gains in SE with time-division duplex operation. It provides array gain with hundreds of antennas at BS and spatial multiplexing gain using space division multiplexing. One of the ways to improve SE is to have perfect CSI at BS and it can be achieved through channel estimation. The channel estimation can be achieved by piloting method. The mutually orthogonal pilots are used by BS to estimate the channel. The precoder and combiner are formulated from channel estimators. The constraint of channel coherence time and frequency leads to trade-off between available resources for data and piloting. However, resources spent on piloting can be reduced by reuse of pilot sequences in nearby cells, called pilot reuse. Eventually, pilot reuse causes potential inter-cell interference during the channel estimation, called pilot contamination. In this article, we analyzed the

FOREX Publication
Open Access | Rapid and quality publishing
International Journal of Electrical and Electronics Research (IJEER)
Research Article | Volume 11, Issue 4 | Pages 1001-1012 | e-ISSN: 2347-470X

impact of pilot reuse factor on sum averaged SE for various channel estimators. The MMSE channel estimator estimates channel mean and whole channel covariance matrix for obtaining Channel State Information (CSI); due to that it is computationally complex but gives best interference cancelation. However, EW-MMSE is estimate channel mean and on diagonal elements of channel covariance matrix; due to that it is less computationally complex but interference cancelation quality is inferior to MMSE. The LS does not obtain any CSI; due to that computational complexity is lowest but interference cancelation quality is lowest among all discussed estimators. The SE is directly proportional to the number of samples available for data transmission in coherent block over which the channel response is time-invariant and frequency-flat. Further, the SE is logarithmically proportional to SINR. The increase in pilot reuse factor causes f times more pilots than number of UEs per cell and it consumes samples in coherent block for piloting, which decreases samples in coherent block for data transmission. As a result, at first look SE decreases as number data bits per second are decreasing, but it is not as simple as looks. The increase in pilot reuse factor also decreases inter-cell interference and as result SINR improves, which manifest the increment of SE. So, there is trade-off between pilot samples and data samples for SE enhancement. As per obtained results, the optimum pilot reuse factor is 4. The SE is decreasing as whole as pilot reuse factor increases, because the SE is directly proportional to the pre-log factor $\tau_{u/d}/\tau_c$ and logarithmically proportional to the SINR. However, the difference between values of SEs for $f = 1$ to $f = 2$ to $f = 4$ are very low and performance difference between estimators is decreasing as pilot reuse factor is increases, which allows to use LS estimator to get performance almost equal to MMSE with less computational complexity.

REFERENCES

[1] LTE; Evolved Universal Terrestrial Radio Access (E-UTRA); Physical layer procedures (3GPP TS 36.213 version 10.3.0 Release 10), ETSI TS 136 213 V10.3.0 (2011-10).

[2] E. Björnson, J. Hoydis, and L. Sanguinetti, "Massive MIMO networks:Spectral, energy, and hardware efficiency," Foundations and Trends® in Signal Processing, vol. 11, no. 3-4, pp. 154–655, 2017.

[3] Luca Sanguinetti, Emil Björnson, and Jakob Hoydis, "Towards Massive MIMO 2.0: Understanding spatial correlation, interference suppression, and pilot contamination", IEEE Transactions on Communications, Vol. 68, Iss. 1, pp. 232 – 257, IEEE, January 2020.

[4] T. L. Marzetta, "Noncooperative cellular wireless with unlimited numbers of base station antennas," IEEE Trans. Wireless Commun., vol. 9, no. 11, pp. 3590–3600, Nov. 2010.

[5] A. Adhikary, A. Ashikhmin, and T. L. Marzetta, "Uplink interference reduction in large scale antenna systems," IEEE Trans. Commun., vol. 65, no. 5, pp. 2194–2206, 2017.

[6] E. Björnson, J. Hoydis, and L. Sanguinetti, "Massive MIMO has unlimited capacity," IEEE Trans. Wireless Commun., vol. 17, no. 1, pp. 574–590, Jan. 2018.

[7] Vidit Saxena, "Pilot Contamination and Mitigation Techniques in Massive MIMO Systems", Thesis, Department of Electrical and Information Technology LTH, Sweden, October, 2014.

[8] Emil Björnson, Erik G. Larsson, and M´erouane Debbah, "Massive MIMO for Maximal Spectral Efficiency:How Many Users and Pilots Should Be Allocated?", IEEE Transactions on Wireless Communications, vol. 15, Iss. 2, pp. 1293 - 1308, IEEE, February 2016.

[9] Özgecan Özdogan, Björnson, and Erik G. Larsson, "Massive MIMO with Spatially Correlated Rician Fading Channels," IEEE Transactions On Communications,v. 67, no. 5, pp. 3234-3250, May 2019.

[10] Li You, Xiqi Gao, Xiang-Gen Xia, Ni Ma, and Yan Peng, "Pilot Reuse for Massive MIMO Transmission over Spatially Correlated Rayleigh Fading Channels", IEEE Transactions on Wireless Communications, vol. 14, Iss. 6, pp. 3352 – 3366, IEEE, June 2015.

[11] Italo Atzeni, Jes´us Arnau, and M´erouane Debbah, "Fractional Pilot Reuse in Massive MIMO Systems", IEEE International Conference on Communication Workshop (ICCW), London, UK, IEEE, 2015.

[12] Rami Mochaourab, Emil Bj¨ornson, and Mats Bengtsson, "Adaptive Pilot Clustering in Heterogeneous Massive MIMO Networks", IEEE Transactions on Wireless Communications, vol. 15, Iss. 8, pp. 5555 - 5568, August 2016.

[13] Yikun Mei and Zhen Gao, "CS-Based CSIT Estimation for Downlink Pilot Decontamination in Multi-Cell FDD Massive MIMO", IEEE/CIC International Conference on Communications in China (ICCC), Xiamen, China, IEEE, 2021.

[14] Jiahui LI, Limin XIAO, Xibin XU and Shidong ZHOU, "Sectorization based pilot reuse for improving net spectral efficiency in the multicell massive MIMO system", Science China Information Sciences, vol.59, pp. 1–15, Science China Press and Springer, 2016.

[15] Wenfeng Li and Xuebin Sun, "Pilot Assignment Based on Weighted-Count for Cell-Free Massive MIMO Systems", Asia-Pacific Conference on Communications Technology and Computer Science (ACCTCS), Shenyang, China, IEEE, 2021.

[16] Olakunle Elijah, Chee Yen Leow, Abdul Rahman Tharek, Solomon Nunoo, and Solomon Zakwoi Iliya, "Mitigating Pilot Contamination in Massive MIMO System - 5G: An Overview", 10th Asian Control Conference (ASCC), Kota Kinabalu, Malaysia, IEEE, 2015.

[17] Yu Hao, Jin Xin, Wang Tao, Song Tao, Lv Yu-xiang, and Wu Hao, "Pilot Allocation Algorithm Based on K-means Clustering in Cell-Free Massive MIMO Systems", IEEE 6th International Conference on Computer and Communications (ICCC), Chengdu, China, IEEE, 2020.

[18] Haifen Yang and Yifeng Chen, "A Pilot Assignment Scheme for Multi-cell Massive MIMO System", International Conference on Electronics, Information, and Communication (ICEIC), Barcelona, Spain, IEEE, 2020.

[19] Zijun Gong, Cheng Li , and Fan Jiang, "Pilot contamination mitigation strategies in massive MIMO systems", The Institute of Engineering and Technology, vol. 11, Iss. 16, pp. 2403-2409, John Wiley & Sons, 2017.

[20] Yonghee Han and Jungwoo Lee, "Uplink Pilot Design for Multi-cell Massive MIMO Networks", IEEE Communications Letters, vol. 20, Iss. 8, pp. 1619 – 1622, IEEE, August 2016.

[21] Mahmoud M. Badr, Mostafa M. Fouda, and Adly S. Tag Eldien, "A Novel Vision to Mitigate Pilot Contamination in Massive MIMO-based 5G Networks", 11th International Conference on Computer Engineering & Systems (ICCES), Cairo, Egypt, IEEE, 2016.

[22] Heng Liu, Shi Jin, and Bo Ai, "Graph Coloring Based Pilot Assignment for Cell-Free Massive MIMO Systems", IEEE Transactions on Vehicular Technology, vol. 69, Iss. 8, pp. 9180 – 9184, August 2020.

[23] Tien Hoa Nguyen, Trinh Van Chien, Hien Quoc Ngo, Xuan Nam Tran, and Emil Björnson, "Pilot Assignment for Joint Uplink-Downlink Spectral Efficiency Enhancement in Massive MIMO Systems with Spatial Correlation", IEEE Transactions on Vehicular Technology, vol. 70, Iss. 8, pp. 8292 – 8297, IEEE, August 2021.

[24] Manobendu Sarker_ and Abraham O. Fapojuwo, "Granting Massive Access by Adaptive Pilot Assignment Scheme for Scalable Cell-free Massive MIMO Systems", IEEE 93rd Vehicular Technology Conference (VTC2021-Spring), Helsinki, Finland, IEEE, 2021.

[25] Li You, Xiqi Gao, Xiang-Gen Xia, Ni Ma, and Yan Peng, "Pilot Reuse for Massive MIMO Transmission over Spatially Correlated Rayleigh Fading Channels", IEEE Transactions on Wireless Communications, vol. 14, Iss. 6, pp. 3352 – 3366, IEEE, June 2015.

[26] Zahra Bahrani, and Mohsen Eslami, "A Least Square Channel Estimator with Pilot Deficit for Multiuser Massive MIMO Downlink", 23rd Iranian Conference on Electrical Engineering, Tehran, Iran, IEEE, 2015.

International Journal of
Electrical and Electronics Research (IJEER)
Research Article | Volume 11, Issue 4 | Pages 1001-1012 | e-ISSN: 2347-470X

[27] Technical Report, 3rd Generation Partnership Project; Technical Specification Group Radio Access Network; Spatial channel model for Multiple Input Multiple Output (MIMO) simulations (Release 17), 3GPP TR 25.996 V17.0.0 (2022-03).